## Fig. S1: XRD patterns of Fmoc-Phe-Gly

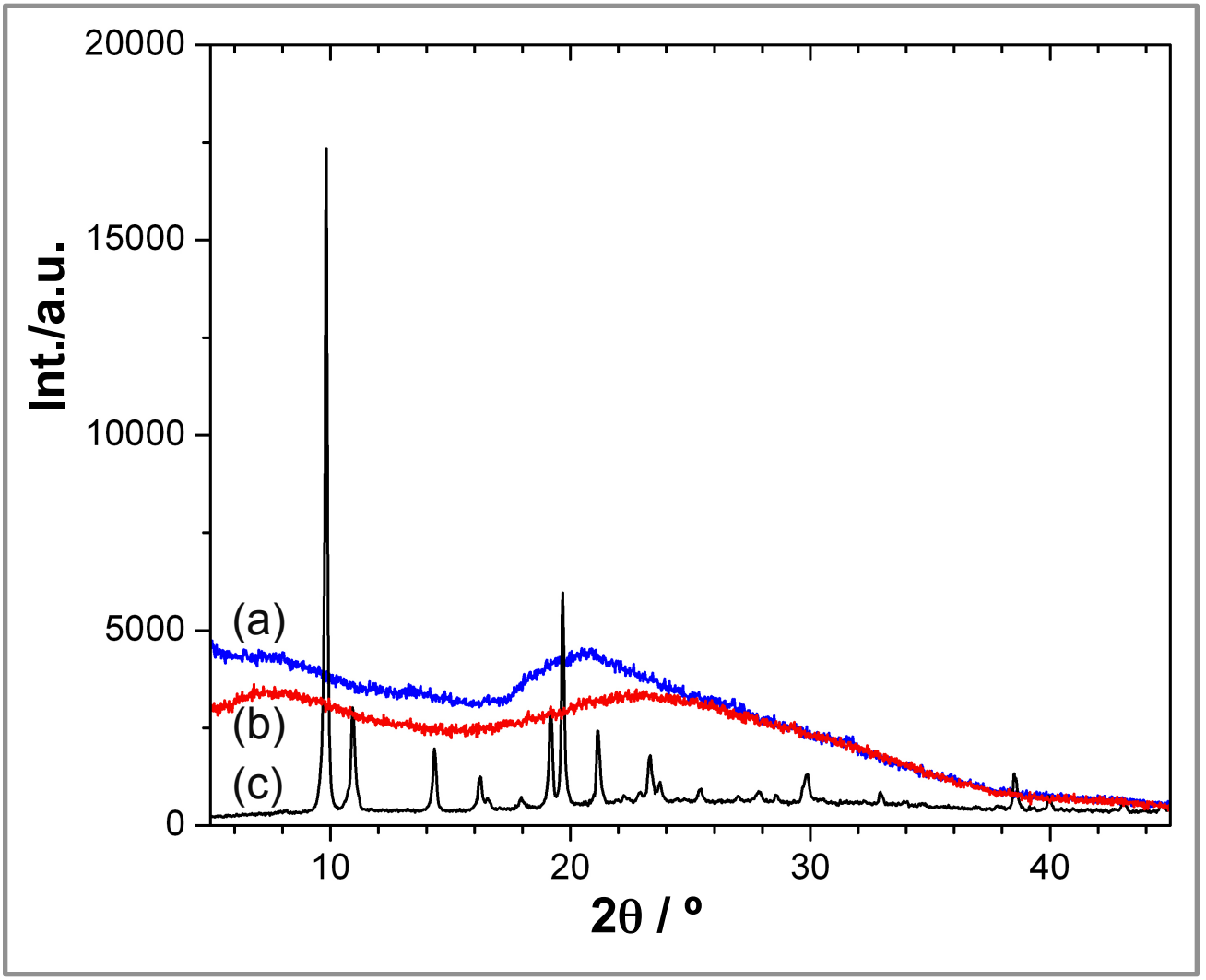


*XRD patterns from (a) Fmoc-Phy-Gly powder sample and (b) electrospun Fmoc-Phe-Gly from HFIP solution (both fibres and small droplets were observed in this sample). The results are compared with a nicely crystalline sample, (c) 9-Fluorenemethanol powder, measured in the same configuration.*

# Fig. S2: Curve fitting of amide I band, IR (ATR) of albumin powder

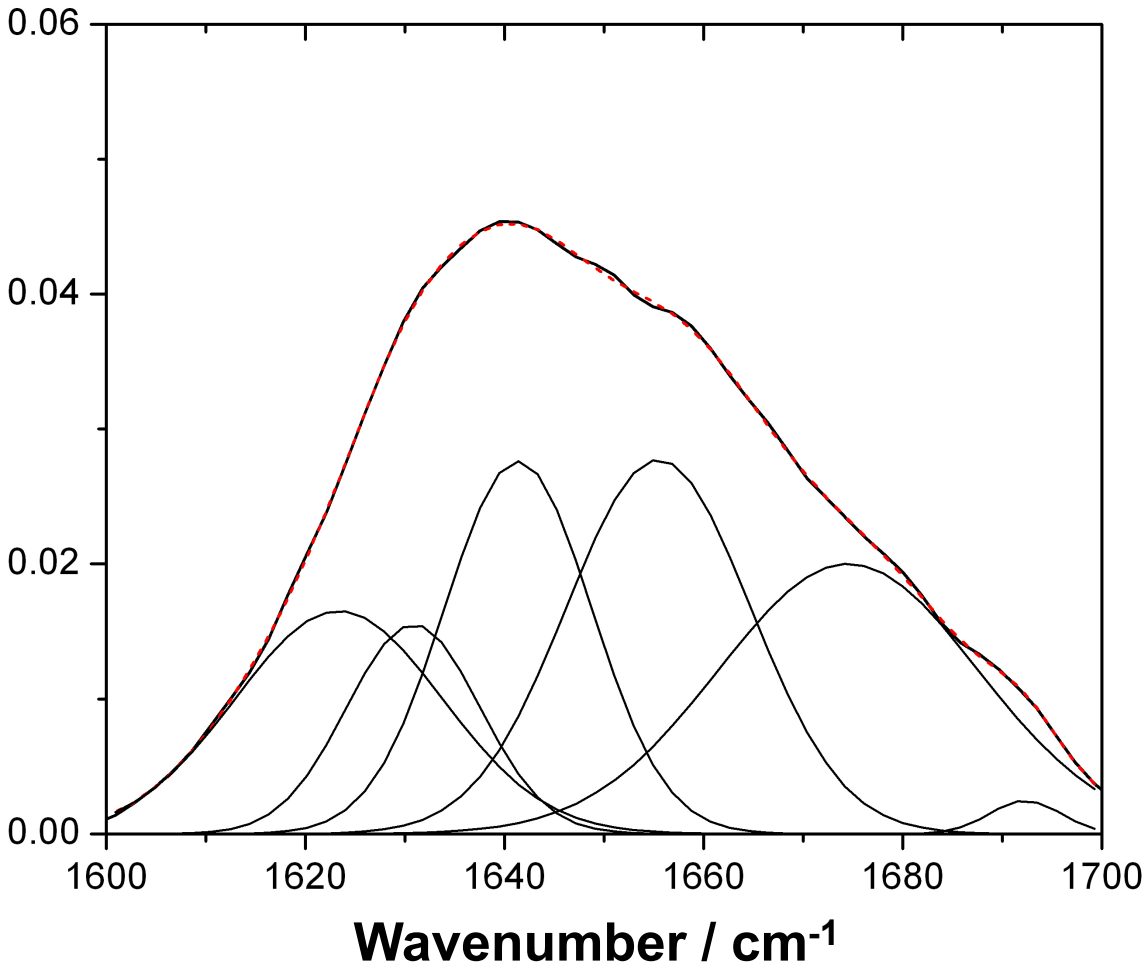


FTIR in ATR mode, at 4 cm-1, 1000 scans

| Peak | Position | Int. | Width | Area | % |
|---|---|---|---|---|---|
| 1 | 1623 | 0.017 | 24.5 | 0.44 | 17 |
| 2 | 1631 | 0.016 | 15.7 | 0.27 | 11 |
| 3 | 1641 | 0.028 | 17.4 | 0.52 | 20 |
| 4 | 1655 | 0.028 | 21.7 | 0.65 | 25 |
| 5 | 1674 | 0.02 | 30.7 | 0.65 | 26 |
| 6 | 1692 | 0.002 | 8.4 | 0.02 | 1 |

The fits were interpreted in terms of secondary structure according to [J. Pelton, L.R. McLean, *Anal. Biochem.*, 2000, **277**, 167], allowing for an error of 5 $cm^{-1}$:
$\alpha$-helices 1650-1657 $cm^{-1}$
$\beta$-sheets 1612-1640 $cm^{-1}$
Turns 1655-1675 and 1680-1696 $cm^{-1}$
Unordered 1640-1651 $cm^{-1}$

Relative fractions of secondary structures are reported with an accuracy of 5%; turns are not specified; sheets are not divided into parallel/antiparallel.

**Fig. S3: Curve fitting of amide I band, IR (ATR) of albumin fibres electrospun from HFIP solution**

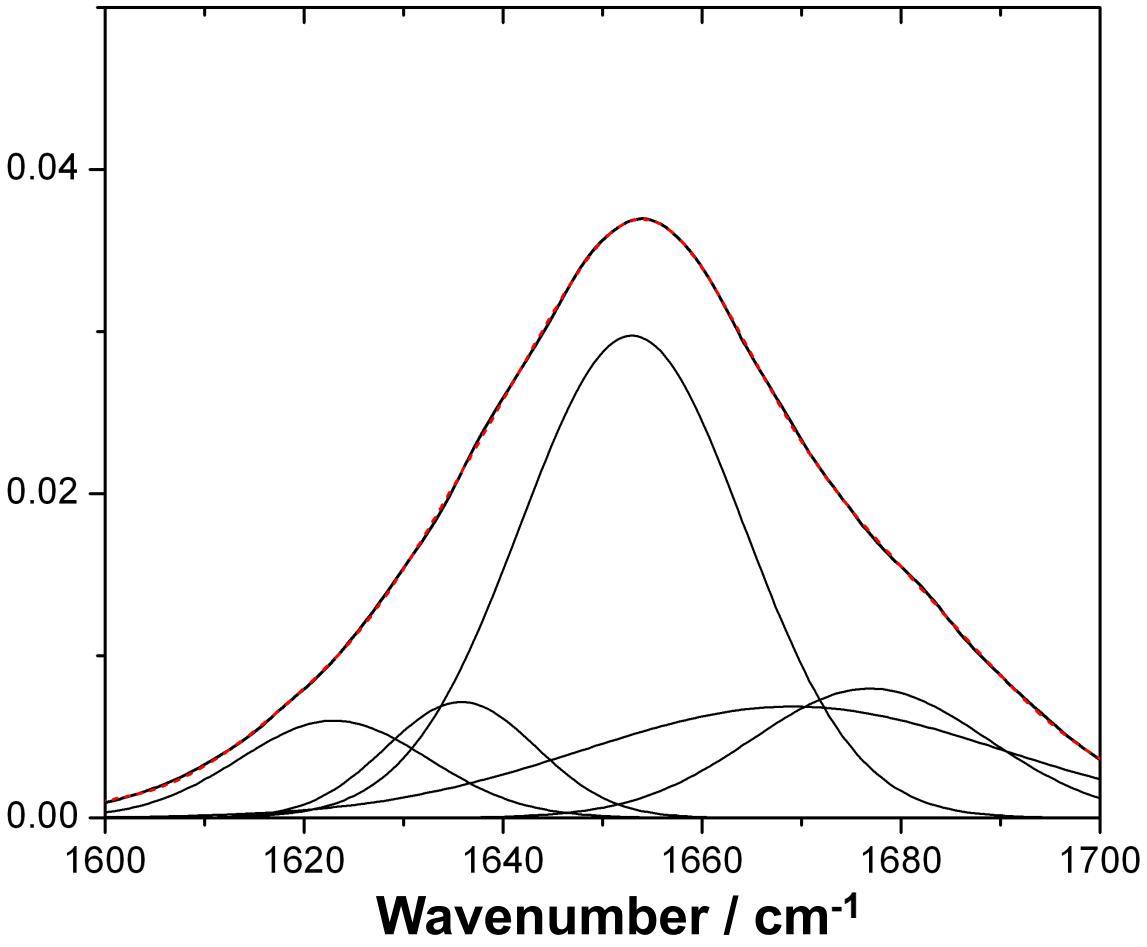


FTIR in ATR mode, at 4 cm-1, 1000 scans

| Peak | Position | Int. | Width | Area | % |
|---|---|---|---|---|---|
| 1 | 1623 | 0.006 | 22.4 | 0.14 | 8 |
| 2 | 1636 | 0.007 | 17.8 | 0.13 | 8 |
| 3 | 1653 | 0.03 | 26.4 | 0.84 | 49 |
| 4 | 1669 | 0.007 | 49.9 | 0.37 | 22 |
| 5 | 1677 | 0.008 | 28 | 0.24 | 14 |

**Fig. S4: Curve fitting of amide I band, IR (ATR) of albumin fibres electrospun from TFA solution**

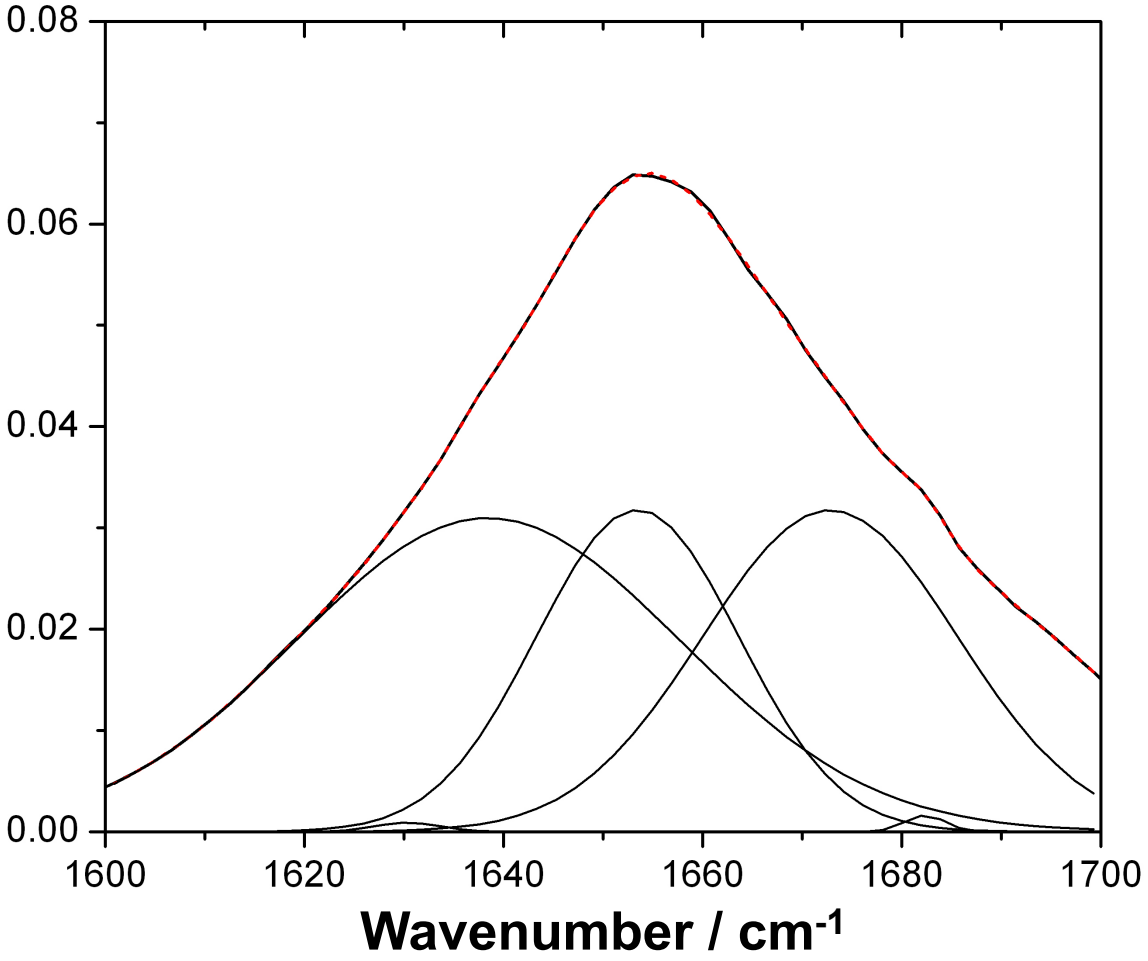


FTIR in ATR mode, at 4 cm-1, 1000 scans

| Peak | Position | Int. | Width | Area | % |
|---|---|---|---|---|---|
| 1 | 1630 | 0.001 | 7.6 | 0.01 | 0 |
| 2 | 1638 | 0.031 | 45.6 | 1.51 | 45 |
| 3 | 1653 | 0.032 | 23.9 | 0.82 | 24 |
| 4 | 1673 | 0.032 | 30.2 | 1.03 | 31 |
| 5 | 1682 | 0.002 | 4.7 | 0.01 | 0 |